Neuron, Vol. 21, 1067–1078, November, 1998, Copyright ©1998 by Cell Press

Activity-Dependent Modulation of Synaptic AMPA Receptor Accumulation

Richard J. O'Brien,*†‡# Sunjeev Kamboj,*†# Michael D. Ehlers,*† Kenneth R. Rosen,§ Gerald D. Fischbach,§ and Richard L. Huganir*†‖

*Howard Hughes Medical Institute
†Department of Neuroscience
‡Department of Neurology
Johns Hopkins University School of Medicine
Baltimore, Maryland 21205
§Department of Neuroscience
Harvard Medical School
Boston, Massachusetts 02110

Summary

Both theoretical and experimental work have suggested that central neurons compensate for changes in excitatory synaptic input in order to maintain a relatively constant output. We report here that inhibition of excitatory synaptic transmission in cultured spinal neurons leads to an increase in mEPSC amplitudes, accompanied by an equivalent increase in the accumulation of AMPA receptors at synapses. Conversely, increasing excitatory synaptic activity leads to a decrease in synaptic AMPA receptors and a decline in mEPSC amplitude. The time course of this synaptic remodeling is slow, similar to the metabolic half-life of neuronal AMPA receptors. Moreover, inhibiting excitatory synaptic transmission significantly prolongs the half-life of the AMPA receptor subunit GluR1, suggesting that synaptic activity modulates the size of the mEPSC by regulating the turnover of postsynaptic AMPA receptors.

Introduction

Neurons maintain an overall homeostatic response to the level of excitatory synaptic transmission. This regulatory process may play a critical role in the modulation of both normal and pathologic neuronal function. It has been proposed that individual neurons act as long-term (over a period of days) integrators of their past synaptic activity and possess mechanisms to compensate for increases or decreases in the level of excitatory synaptic input (see Bear, 1995; Miller, 1996). This activity-dependent adjustment in the output strength of the postsynaptic neuron may be important in setting the threshold for the induction of long-term potentiation (LTP) and long-term depression (LTD). Changes in neuronal activity that have a long-term impact on the cell's output may also have important roles in disease processes. For example, Furshpan and Potter (1989) have shown that blockade of excitatory synaptic transmission predisposes neurons to bursting synaptic activity and excitotoxic cell death due to the induction of local circuit epileptiform activity.

We have previously reported that blockade of excitatory synaptic transmission in cultured spinal neurons results in an increase in the glutamate chemosensitivity of the postsynaptic neuron (O'Brien and Fischbach, 1986). Segal and Furshpan reported that this same blockade resulted in large excitatory synaptic potentials and epileptic discharges in cultured hippocampal neurons (1990). Recently, Turrigiano et al. (1998) have reported that blocking excitatory synaptic transmission in cortical neurons results in increased mEPSC amplitudes and increased postsynaptic glutamate sensitivity. Postsynaptic ionotropic glutamate receptors are composed of three broad classes, termed AMPA, NMDA, and kainate type receptors, on the basis of molecular and pharmacological criteria (Hollmann and Heinemann, 1994). The predominant charge carrier during routine fast excitatory synaptic transmission is the AMPA type receptor, while NMDA receptors contribute a significant calcium current, which is thought to modulate second messenger systems and kinases. To date, experiments have suggested that the increased mEPSC amplitude and neuronal glutamate sensitivity resulting from the blockade of excitatory synaptic activity are due to an alteration in the AMPA class of receptors (O'Brien and Fischbach, 1986; Turrigiano et al., 1998), although one recent report also noted an effect on NMDA receptor distribution (Rao and Craig, 1997). Whether the activity-regulated increase in postsynaptic glutamate sensitivity results from a change in the number of postsynaptic AMPA receptor subunits or from a change in their single channel properties is unclear. Precedents for both mechanisms exist. Recent work on inhibitory synapses in the cerebellum has suggested that postsynaptic $GABA_A$ receptor number can determine quantal size (Nusser et al., 1997), while work from our own lab has shown that receptor phosphorylation can modulate channel gating (see for example Roche et al., 1996; Traynelis and Wahl, 1997). In addition, the onset of axonal sprouting and de novo synaptogenesis, which is influenced by synaptic activity (Cline and Constantine-Paton, 1990), may also alter postsynaptic neuronal glutamate sensitivity.

We report here that alterations in the amount of excitatory synaptic transmission present in cultured spinal neurons result in a significant change in the amplitude of mEPSCs, an effect that can be quantitatively accounted for by the size of immunostained postsynaptic AMPA receptor clusters. The time course and magnitude of this effect are a reflection of the turnover of synaptic AMPA receptors whose metabolic half-life is modulated by excitatory synaptic activity. These results indicate that neuronal activity modulates excitatory synaptic transmission by regulating the accumulation of AMPA receptors at synapses through a novel signaling pathway.

Results

Synaptic Activity Regulates mEPSC Amplitude

To investigate the effect of synaptic activity on the efficacy of excitatory synaptic transmission, cultured spinal

‖To whom correspondence should be addressed (e-mail: rick.huganir@qmail.bs.jhu.edu).

#These authors contributed equally to this work.

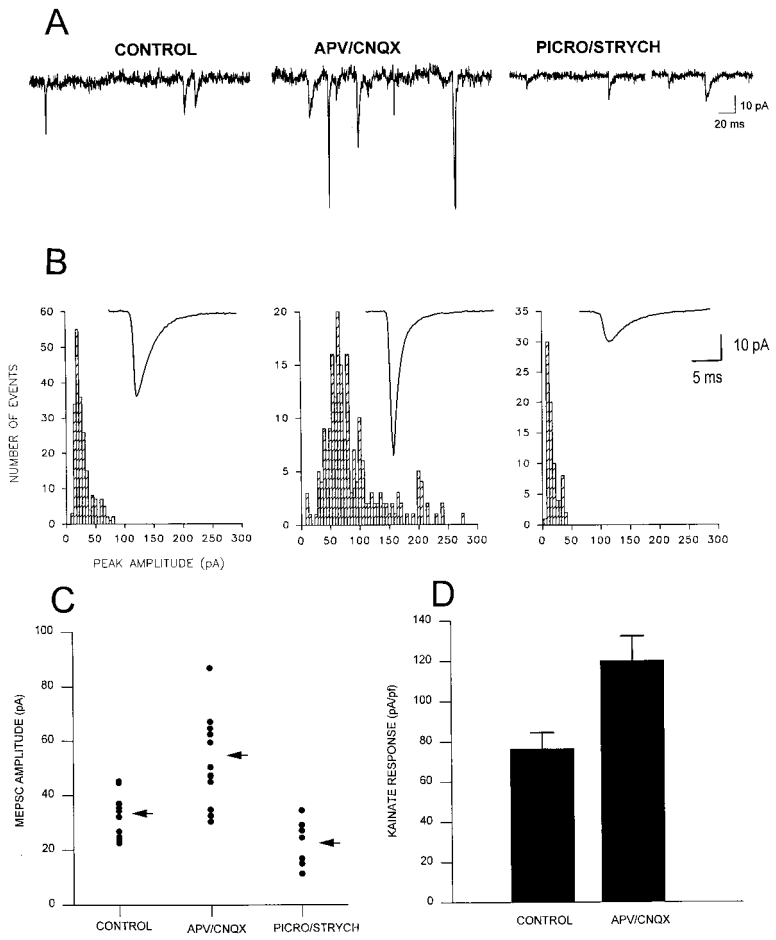

Figure 1. Excitatory Synaptic Activity Modulates mEPSC Amplitude

(A) MEPSCs recorded from representative control (left panel), inhibited (middle panel), and active cells (right panel). The calibration bars apply to all traces.

(B) Typical amplitude histograms from individual control, inhibited, and active cells (the bin width is 5 pA for all histograms). The insets show average mEPSC waveforms corresponding to the displayed histogram.

(C) Mean mEPSC amplitudes from a series of individual control (n = 11), inhibited (n = 12), and active (n = 7) neurons are shown. Each mean differs from the other two at the 0.05 level (t test).

(D) The mean kainate sensitivity (normalized to cell capacitance) from a subset of control and inhibited neurons (n = 7 control; n = 8 inhibited [$p < 0.03$]).

neurons were incubated with either glutamate receptor antagonists to block excitatory synaptic transmission or with $GABA_A$ and glycine receptor antagonists to increase basal excitatory synaptic activity. The cells were initially maintained in culture in the absence of receptor antagonists for 1 week, at which time spontaneous excitatory synaptic transmission is widespread. The cells were then incubated for a subsequent 3 days in either control media (control cells), media containing the glutamate receptor antagonists CNQX and APV (inhibited cells), or media containing the $GABA_A$ and glycine receptor antagonists picrotoxin and strychnine (active cells). Previous work has shown that CNQX (10 μM) and APV (300 μM) are completely effective at blocking AMPA and NMDA receptor–mediated synaptic transmission in these cultures (O'Brien et al., 1997). In contrast, picrotoxin (100 μM) and strychnine (2 μM) eliminate the large inhibitory currents normally present in these cultures (Choi et al., 1981; O'Brien et al., 1997), allowing the EPSCs to more easily summate to produce postsynaptic depolarization and spiking (Choi et al., 1981; Turrigiano et al., 1998). Following the 72 hr treatment, AMPA receptor–mediated mEPSCs were recorded in the presence of TTX (1 μM), picrotoxin (100 μM), strychnine (1 μM), and APV (50 μM). These mEPSCs exhibited rapid 10%–90% rise times of <2 ms and typically decayed with a single exponential time constant of <5 ms. Figure 1A shows mEPSCs recorded from a control cell, an inhibited cell, and an active cell, while mEPSC amplitude histograms from these same three cells are shown in Figure 1B. Chronic inhibition of excitatory synaptic transmission dramatically increased the mean mEPSC amplitude from a control value of 33.0 ± 2.4 pA (SEM, n = 11) to 52.9 ± 4.7 pA (SEM, n = 12). In contrast, increasing the level of excitatory synaptic activity with picrotoxin and strychnine decreased the mean mEPSC amplitude to 22.5 ± 3.0 pA (SEM, n = 7). Under all conditions, the amplitude histograms were skewed toward higher values, as previously described for other central synapses (see Jack et al., 1994; Walmsley, 1995). It is unlikely that the skew we observe arises as a result of differences in the electrotonic distance of synapses from the somatic recording site, since no correlation was found between the kinetics of mEPSCs (measured by their 10%–90% rise times or decay times) and their amplitudes. The mean mEPSC amplitudes for individual cells under the three conditions are shown in Figure 1C. Comparing the chronically inhibited cultures (APV/CNQX) to the chronically active cultures (picrotoxin/strychnine), the range of the response of mEPSCs to changes in excitatory synaptic activity was 2.35-fold (Figure 1C). No significant difference in the frequency or kinetics of mEPSCs was observed between the three conditions, and the series resistance and capacitance of

Table 1. The Effect of Snyaptic Activity on the Accumulation of AMPA Receptors at Excitatory Synapses

	The Effect of Synaptic Activity on Synapse Number and Neuronal Survival			The Effect of Snyaptic Activity on Mean Synaptic Fluorescence Intensity			
	GluR1 Clusters/Neuron	Synapses/ Neuron	Neurons (63× Field)	N GluR1	C GluR1	GluR2	Synaptophysin
Control cultures	13.6 ± 6.1	26.1 ± 8.9	10 ± 4.8	5993 ± 2502	6208 ± 1819	4469 ± 1261	7811 ± 2397
+ Picro/Strych	14.7 ± 4.5	22.7 ± 7.1	11.8 ± 5.1	3587 ± 822	3959 ± 879	2883 ± 814	7873 ± 2214
+ APV/CNQX	12.1 ± 4.2	23.8 ± 11.1	9.2 ± 5.3	10076 ± 2008	10591 ± 3132	7621 ± 2101	7527 ± 1998

Control, inhibited, and active cultures were grown as described in Experimental Procedures. On day 10 in vitro, separate coverslips were double stained for C-GluR1 (Cy3) and synaptophysin (FITC) and viewed with a 63× objective. Each number represents data (± SD) from ten neurons or visual fields in each of six platings. In addition, the mean neuronal synaptic fluorescence intensities for N-GluR1, C-GluR1, N-GluR2, and synaptophysin were calculated for a series of neurons in each of the three experimental conditions as described in the legend to Figure 3.

the cells remained unchanged. As described previously, the mEPSCs appeared to lack a slower component, corresponding to NMDA receptor activation, even in the presence of 1 μM glycine and low Mg^{2+} (O'Brien et al., 1997).

The increase in mEPSC amplitude seen in chronically inhibited neurons was accompanied by a corresponding increase in neuronal glutamate sensitivity. Application of kainate (1 mM) produced significantly larger responses in inhibited cells than in control cells. As summarized in Figure 1D, kainate-evoked responses (normalized to the cell's capacitance) in control cells had a mean amplitude of 76.5 ± 8.3 pA/pF (SEM, n = 8), whereas inhibited cells had a mean amplitude of 120.0 ± 12.6 pA/pF (SEM, n = 7). The effect of synaptic activity on mEPSC amplitude and kainate sensitivity occurred in the absence of any change in the neuronal density, the number of total synapses per neuron, or the number of AMPA receptor clusters per neuron (Table 1).

Synaptic Activity Regulates the Accumulation of AMPA Receptors at Synapses

Taken together, these results suggest that changes in the synaptic activity of cultured spinal neurons results in a postsynaptic alteration in AMPA receptor function. Since an alteration in mEPSC amplitude and kainate sensitivity could be due to either a change in the number of synaptic AMPA receptors or to a change in their single channel properties, we sought to quantitate the accumulation of AMPA receptors at individual postsynaptic sites. Given that the surface expression of synaptic AMPA receptors may be a variable portion of the total population (Mammen et al., 1997), it was important to examine both the intracellular and surface pools of synaptic AMPA receptors independently. To specifically examine surface AMPA receptors, we labeled live neurons with an antibody generated against the extracellular N-terminal region of GluR1 (N-GluR1; Mammen et al., 1997). An antibody generated against the intracellular C terminus of GluR1 (C-GluR1; O'Brien et al., 1997) was applied, after fixation and permeabilization, to label both surface and subsurface pools of GluR1. When used in this manner and quantitated as described in Experimental Procedures, the distribution of fluorescence intensities of postsynaptic AMPA receptor clusters on individual neurons showed a skewed pattern, similar to the distribution of mEPSC amplitudes (Figure 2). In addition, there was a tight correlation between the intensity of N-GluR1 and C-GluR1 staining (mean correlation coefficient = 0.85 ± 0.06, n = 4), suggesting that our assay is sensitive to physiologic differences in synaptic AMPA receptor concentration.

To investigate the relationship between synaptic activity and postsynaptic AMPA receptor clustering, we examined postsynaptic GluR1 clusters, using both double and triple staining techniques, in a series of control, inhibited, and active neurons. For double staining, we combined either C-GluR1 (total synaptic GluR1), N-GluR1 (surface synaptic GluR1), or GluR2 (total synaptic GluR2; Vissavajjhala et al., 1996) staining with FITC-labeled synaptophysin staining. For triple staining, surface GluR1 (FITC-labeled N-GluR1), total GluR1 (CY3-labeled C-GluR1), and synapses (AMCA-labeled synaptophysin) were identified simultaneously as described in Experimental Procedures. Both techniques gave identical results, and the data were pooled. As shown in Figure 3 and quantified in Table 1, inhibition of excitatory synaptic transmission increased the size and fluorescence intensity of the signals corresponding to the surface (N-GluR1) and total (C-GluR1) pools of postsynaptic AMPA receptors compared to control cultures. Moreover, increasing excitatory synaptic activity with picrotoxin and strychnine decreased the size and fluorescence intensity of the signals corresponding to postsynaptic AMPA receptor clusters. A similar effect was seen for GluR2 (Table 1). The effect of synaptic activity on postsynaptic AMPA receptor accumulation occurred in the absence of any change in the size or fluorescence intensity of the signal from the synaptic vesicle protein synaptophysin (Figure 3 and Table 1) or in the diffuse intradendritic C-GluR1 staining (control, 29 ± 8 U; inhibited, 30 ± 9 U; active, 33 ± 11 U). Comparing chronically inhibited cultures (APV/CNQX) to chronically active cultures (picrotoxin/strychnine), the range of the response of synaptic AMPA receptor accumulation to changes in excitatory synaptic activity was 2.83 ± 0.23 fold (mean ± SD of GluR2, N-GluR1, and C-GluR1 effect, taken from Table 1). This compares well to the range of mEPSC amplitudes over these same conditions (2.35-fold, Figure 1). The alteration in postsynaptic GluR1 fluorescence intensity was accompanied by a change in the size of the postsynaptic GluR1 fluorescence signal measured with the C-GluR1 antibody (control, 122 ± 29 pixels; inhibited, 173 ± 39 pixels; active, 58 ± 18 pixels). Whether this represents an actual change in the size of the postsynaptic cluster or a spillover of the increased signal is unclear. As mentioned previously, the effect of synaptic activity on

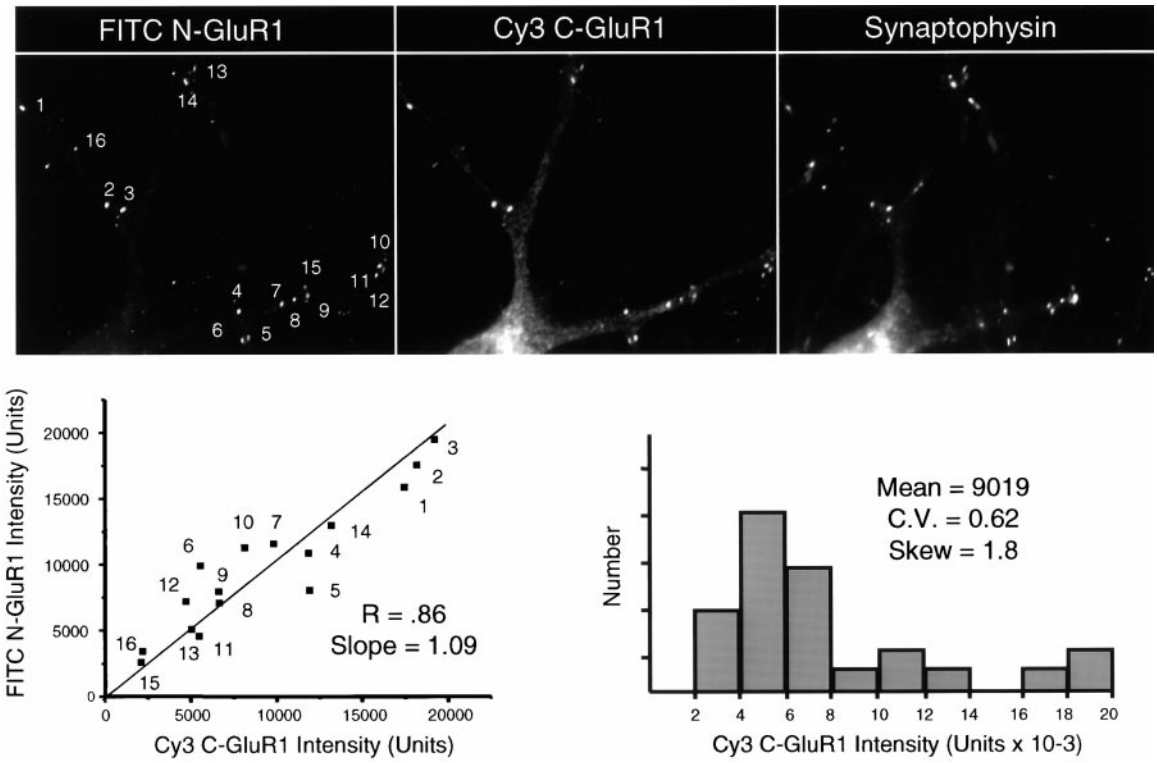

Figure 2. Quantitative Fluorescence Microscopy of Synaptic AMPA Receptor Clusters

(Top) Individual synaptic clusters of GluR1 were digitized as described in Experimental Procedures, and the total synaptic intensity for both N-GluR1 (left panel) and C-GluR1 (middle panel) was quantified at each synapse, identified with the synaptic vesicle protein synaptophysin (right panel).

(Bottom) The total fluorescence intensity for both Cy3 (C-GluR1) and FITC (N-GluR1) at individually numbered synapses is plotted (left panel) and shows the tight and linear correlation between the two. Plotting the mean peak intensity rather than the total intensity gave a similar result. Also evident in this single neuron (right panel) is the clustering of synaptic fluorescence intensities toward the lower end (2,000–8,000), with a broad, skewed (mean/mode) distribution toward higher values (8,000–20,000).

AMPA receptor accumulation occurred in the absence of any change in the survival of neurons, the number of synaptic GluR1 clusters per neuron, or the total number of synapses per neuron (Table 1). The effect of synaptic activity on AMPA receptor cluster size did not occur rapidly but took at least 36 hr to develop (see below).

Although the mean fluorescence intensity of individual postsynaptic AMPA receptor clusters changed in response to alterations in synaptic activity, the shape of the histogram of individual synaptic GluR1 fluorescence intensities did not (Figure 4A). The skewed distribution of postsynaptic AMPA receptor fluorescence intensities seen in individual neurons (Figure 2 and Table 2) was also apparent in these groups of neurons (Figure 4 and Table 2) and is similar to the skewed distribution of mEPSC amplitudes (Figure 1 and Table 2). This suggests that at least part of the skewed distribution of mEPSC amplitudes is due to the skewed distribution of AMPA receptors at individual synapses and that postsynaptic receptor number is limiting for mEPSC amplitude. While this model relies on the assumption that synaptic glutamate concentrations are near saturation (Bruns and Jahn, 1995), it would help explain how changes in postsynaptic receptor number directly affect mEPSC amplitudes.

While the distribution of synaptic AMPA receptor fluorescence intensities was decidedly non-Gaussian, the ratio of surface GluR1 to total GluR1 at individual synapses was well fit by a Gaussian curve in control, inhibited, and active cultures (Figure 4B). In addition, the slope of the ratio of surface/total synaptic GluR1 (FITC/Cy3) and the regression coefficient for this fit are similar in all three conditions. The shape of the Gaussian curves, although modestly different in inhibited neurons, was not statistically different from controls ($p = 0.19$). The simplest explanations for these observations is that most synaptic AMPA receptors are on the surface of the postsynaptic neuron, or that there is a fixed ratio of surface to subsurface receptors at all excitatory synapses which does not vary with the amount of excitatory input.

The Kinetics of Activity-Dependent AMPA Receptor Accumulation

To investigate the time course and reversibility of the activity-dependent modulation of synaptic GluR1 accumulation, we returned chronically inhibited cultures to control glial conditioned medium and followed the decline in the mean synaptic GluR1 fluorescence intensity over time. As shown in Figure 5A, the level of synaptic C-GluR1 fluorescence intensity returned to baseline only after 36 hr in control medium. It is interesting to note that the mean synaptic GluR1 intensity at 36 hr was less

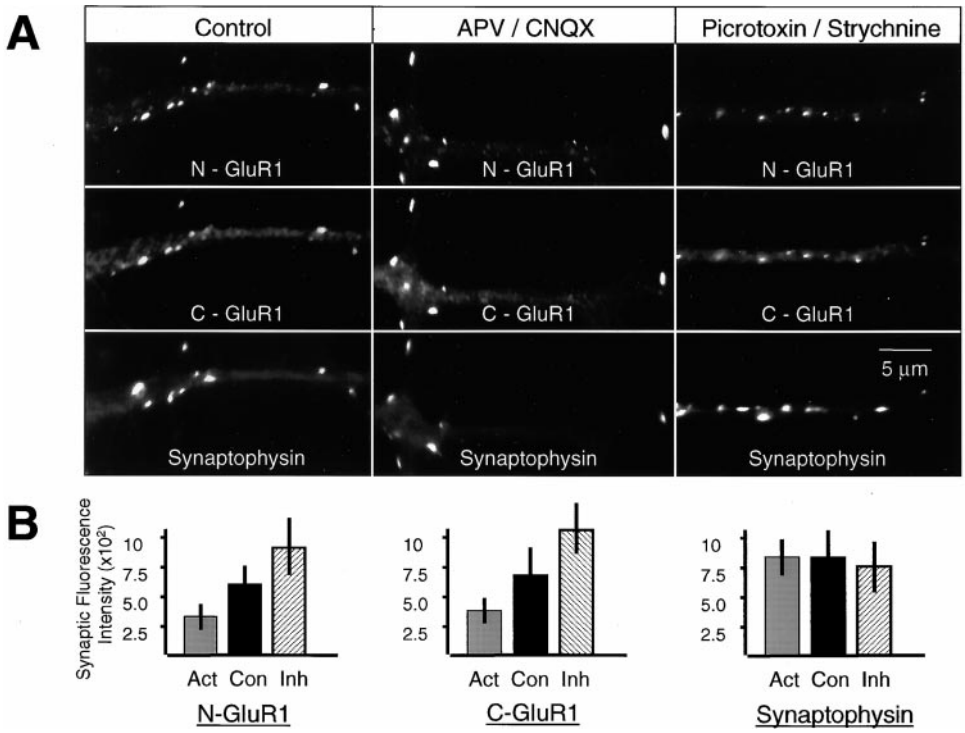

Figure 3. Excitatory Synaptic Activity Modulates the Accumulation of Synaptic AMPA Receptors

(A) Spinal neurons grown for 72 hr in control media, APV and CNQX, or picrotoxin and strychnine, were stained for surface (FITC N-GluR1) and total (CY3 C-GluR1) synaptic GluR1 as described in Experimental Procedures. Associated staining for the synaptic vesicle protein synaptophysin is included to demonstrate the location of synapses. The images displayed were selected because their mean synaptic intensities approached the mean intensities for the experiments as a whole. All images were subjected to the same postacquisition processing. (B) The mean summed neuronal synaptic fluorescence intensity (± SD) for N-GluR1, C-GluR1, and synaptophysin from at least 50 control, active, and inhibited spinal cord neurons is shown. Each bar represents neurons from four separate platings (two using a triple staining technique, two using a double staining technique) and is expressed ± SD. Each bar graph within a plot is different from the other two at the 0.03 level (t test), except for the synaptophysin data.

than the control value ($p = 0.04$), an indication, perhaps, that the increased synaptic activity resulting from the withdrawal of APV and CNQX (see below) transiently drives the expression of synaptic GluR1 to a lower level. The withdrawal of APV and CNQX was not associated with any change in the number of surviving neurons or their synapses, as long as the fresh media had been preincubated with glia for at least 6 hr, presumably both to condition the media and to reduce ambient glutamate levels.

We next sought to determine whether acute increases in excitatory synaptic activity could affect the distribution of GluR1 on a time scale shorter than that described above. To evaluate this, APV and CNQX were withdrawn from chronically inhibited cultures, and the neurons were incubated for 90 min in culture media containing picrotoxin (100 μM) and strychnine (1 μM) to block $GABA_A$ and glycine receptors. This paradigm resulted in sustained rhythmic depolarizing bursts (Figure 5B, arrows), similar to the epileptiform type discharges seen by Furshpan and Potter (1989) in chronically inhibited hippocampal neurons. Following the 90 min period of high synaptic activity, including a 30 min live incubation with N-GluR1, cultures were fixed and stained for surface and total synaptic GluR1 and compared to cultures continuously treated with APV and CNQX. Despite the intense excitatory synaptic activity, we saw no difference in the mean neuronal synaptic N-GluR1 or C-GluR1 staining intensity compared with cultures that had remained in APV and CNQX over the same time period (Figure 5C). Moreover, there was no change in the number of synaptic GluR1 clusters seen on neurons after the 90 min of intense synaptic activity (10.9 ± 3.4 [$n = 2 \times 20$] vs. 11.7 ± 4.8 [$n = 2 \times 20$]). Analysis of a series of individual synapses in acutely active cultures (Figure 5D) showed no change in the ratio of surface to total GluR1, measured using regression analysis, or in the coefficient of variation of the individual synaptic intensities. Using a combination of Z testing, 95% confidence intervals, and modeling, our data could have excluded a 20% change in either the mean surface GluR1 accumulation or the ratio of surface to total synaptic GluR1. In addition, the slope of the regression coefficient was sensitive to a 50% change in the amount of surface receptors in a subpopulation of 30% of the excitatory synapses. Similar results were seen when control cultures (never exposed to APV and CNQX) were incubated with strychnine and picrotoxin for 90 min (data not shown).

Synaptic Activity Regulates the Metabolic Half-Life of AMPA Receptor Subunits

We were interested in whether the effect of synaptic activity on GluR1 localization was associated with a

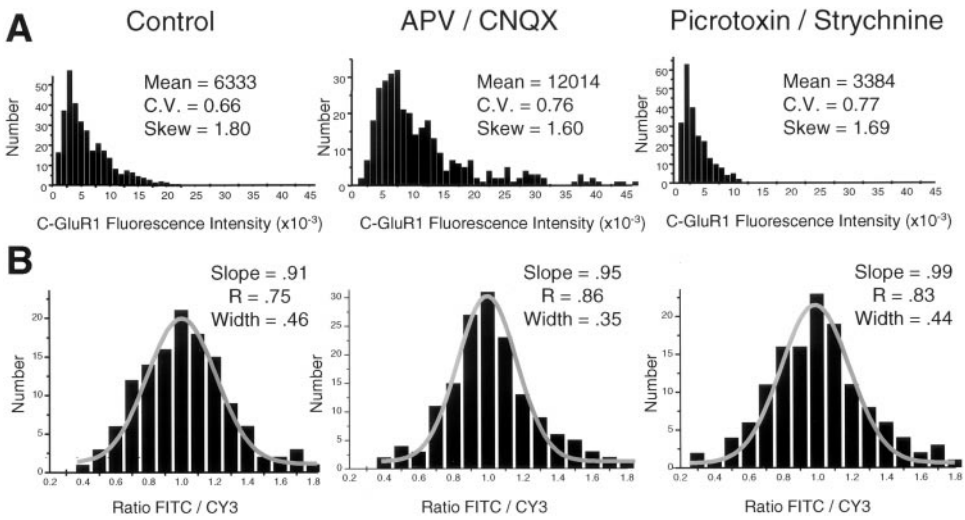

Figure 4. Quantifying the Effect of Synaptic Activity on the Accumulation and Distribution of Synaptic AMPA Receptors

The synaptic fluorescence intensity for N-GluR1 and C-GluR1 was determined in a series of control (n = 29), active (n = 27), and inhibited (n = 20) neurons from the same plating. The fluorescence intensity histograms of individual C-GluR1 clusters are displayed along with their mean, skew (mean/mode), and coefficient of variation (SD/mean). In (B), the ratio of surface to total receptor (FITC/CY3) at individual synapses on ten neurons in each condition (those with the largest number of individual synaptic GluR1 clusters) was analyzed. Each is best fit with a Gaussian distribution whose width is shown. Also shown are the slope and the regression coefficient of the relation between surface and total receptors for each culture condition.

change in total population of neuronal AMPA receptors or was merely a reflection of a redistribution of preexisting receptors. As shown in Figure 6A and Table 3, when assayed by immunoblotting, chronic inhibition of excitatory synaptic transmission caused a net increase in the total amount of GluR1 compared to control cultures, while picrotoxin and strychnine caused a decrease in total GluR1. The magnitude of this effect is similar to that seen in the immunocytochemical and electrophysiological experiments. The effect of synaptic activity on the level of total GluR1 appeared specific, in that there was no change in the amount of tubulin (Figure 6A and Table 3), or total protein (Table 3), and only a modest increase in the level of the AMPA receptor–associated protein GRIP in active cultures. The increase in AMPA receptor subunit accumulation seen in chronically inhibited cultures is not due to an increase in mRNA levels, as Northern blots of control vs. inhibited cultures showed no change in the level of the 5.5 kb GluR1 mRNA transcript (Patneau et al., 1994) when normalized to GAPDH (Figure 6B and Table 3).

In order to investigate the mechanism underlying the activity-dependent accumulation of GluR1, we measured the turnover of GluR1 in the presence and absence of synaptic activity. Previous work had shown that the metabolic half-life of AMPA receptors measured with ^{35}S labeling closely parallels the half-life of synaptic receptors measured by surface biotinylation (Mammen et

Table 2. Synaptic Activity Does Not Alter the Skewed Distribution of Either mEPSC Amplitudes or Synaptic GluR1 Clusters

The Effect of Synaptic Activity on the Pattern of Postsynaptic GluR1 Accumulation						
	Control		APV + CNQX		Picrotoxin and Strychnine	
	Individual	Group	Individual	Group	Individual	Group
C.V.	0.60 ± .09	0.59 ± .05	0.63 ± .11	0.67 ± .1	0.72 ± .1	0.68 ± .12
Skew	1.66 ± .28	1.71 ± .06	1.54 ± .26	1.63 ± .04	1.66 ± .31	1.57 ± .15
The Effect of Synaptic Activity on The Pattern of mEPSC Amplitudes						
C.V.	0.47 ± .09		0.56 ± .08		0.56 ± .34	
Skew	1.31 ± .13		1.50 ± .16		1.42 ± .12	

Synaptic C-GluR1 clusters from neurons in each experimental condition were quantitated and arrayed in aggregate amplitude histograms similar to Figure 4A (Group). The coefficient of variation (SD/mean) and the skew (mode/mean) of the grouped synaptic GluR1 fluorescence intensities from 20 neurons in each of two separate platings were calculated and are displayed ± SD. In addition, the individual amplitude histograms from ten neurons within each experimental condition, selected on the basis of their large number of C-GluR1 clusters, were also constructed, as in Figure 2 (Individual). From these histograms, the skew and coefficient of variation of each of these individual neurons were calculated. Of the 30 individual neurons evaluated, 25 had a clear rightward skew. Finally, the skew and CV of the mEPSC amplitudes recorded from five neurons in each experimental condition are also displayed. The five neurons in each group to be analyzed were again selected on the basis of their large number of mEPSCs.

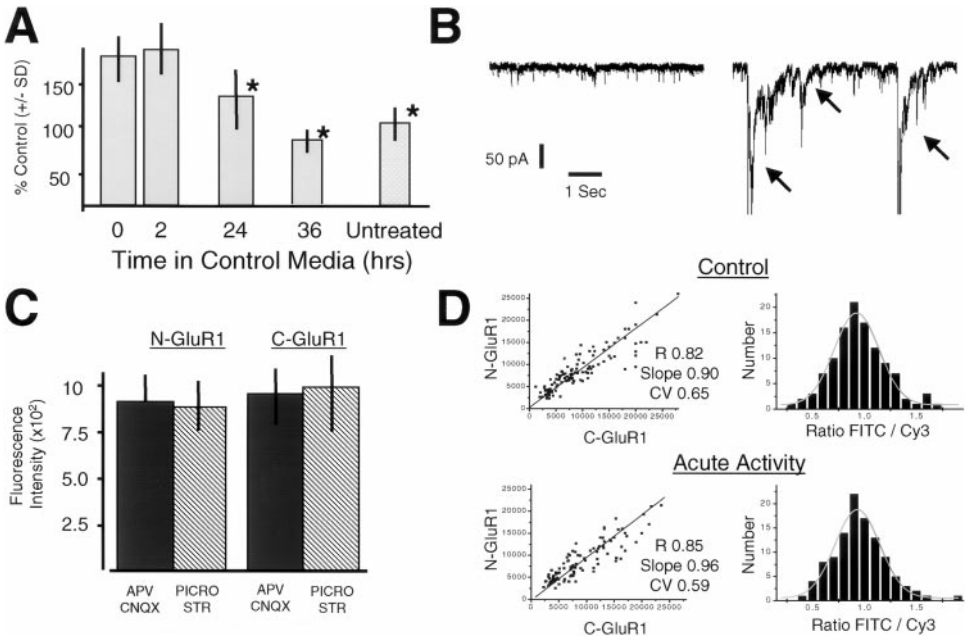

Figure 5. The Time Course of Synaptic GluR1 Remodeling

(A) Neurons treated with APV and CNQX for 72 hr were returned to glial conditioned growth media without inhibitors. After the specified times, cultures were fixed and stained with the C-GluR1 antibody to measure total synaptic GluR1 fluorescence. Each bar represents the mean summed neuronal synaptic GluR1 fluorescence intensity (± SD) taken from 15–20 randomly selected neurons in two distinct platings. The asterisk represents a $p < 0.05$ compared to the preceding time point. The difference between the 36 hr time point and the untreated controls is also significant ($p = 0.04$).

(B) A typical example is shown of the intense, spontaneous, grouped (arrows), excitatory synaptic activity observed following withdrawal from chronic APV and CNQX treatment. A similar trace from a control culture is shown for comparison.

(C) The lack of effect of 90 min of intense excitatory synaptic activity on the mean neuronal synaptic GluR1 signal from 16 neurons continuously treated with APV/CNQX and 17 neurons exposed to picrotoxin and strychnine following 72 hr of chronic inhibition is shown. The data are expressed in absolute units ± SD. The neurons were randomly selected from two separate platings.

(D) The N-GluR1 and C-GluR1 signal from all the individual synapses used in (C) are displayed as a regression analysis and a frequency plot.

al., 1997). As shown in Figures 6C and 6D, the metabolic half-life of GluR1 is significantly prolonged in chronically inhibited cultures compared with controls (31.7 ± 5.9 vs. 18.4 ± 1.5 hr [n = 4; ± SD]). The prolongation of the receptor half-life suggests that increased protein stability is the primary mechanism underlying the increased accumulation of GluR1 in inhibited cultures. Moreover, the half-life of GluR1 in control cultures is similar to the time course for the remodeling of synaptic AMPA receptors in response to excitatory synaptic activity (Figure 5). Of note, the control half-life of GluR1 in these experiments is shorter than that reported previously (Mammen et al., 1997), reflecting differences in experimental conditions, such as the composition of the growth medium, the frequency of media changes, and the age of the neurons.

The Accumulation of Synaptic AMPA Receptors Is Regulated Predominantly by AMPA Receptor Activation

To investigate the pharmacology of activity-regulated synaptic AMPA receptor accumulation, we digitized and quantified a series of C-GluR1, GluR2, and GluR2/3 clusters from 15–20 randomly selected neurons in sister cultures treated either with control media or with APV, CNQX, or TTX. The GluR2/3 antibody recognizes the C-terminal fragment common to both GluR2 and GluR3 (Martin et al., 1993). As can be seen in Figure 7A, CNQX caused a large increase in the synaptic accumulation of AMPA receptors measured by GluR1, GluR2, and GluR2/3 immunostaining. Although TTX caused an increase in synaptic GluR1, it was not as pronounced as CNQX. APV alone had little effect on synaptic AMPA receptor accumulation. The ability of CNQX to regulate the expression of the AMPA receptor subunit GluR2 makes it unlikely that calcium-permeable AMPA receptors are mediating the effect of synaptic activity on AMPA receptor accumulation.

Despite its effect on the synaptic clustering of AMPA receptors, we found that CNQX treatment had no effect on NMDA receptor distribution in cultured spinal neurons. Consistent with our mEPSC data and previously reported results (O'Brien et al., 1997), we found that NR1, an NMDA receptor subunit common to all NMDA receptors, remained diffusely distributed in CNQX-treated neurons (Figure 7B). In contrast, APV treatment (Figure 7C) resulted in the synaptic accumulation of NR1 in a subpopulation of cultured spinal neurons (44 neurons with clustered NR1 out of 204 examined in two platings). This observation is similar to but less extensive than the effect seen by Rao et al. (1997) in cultured hippocampal neurons. We saw no effect of CNQX or APV on the

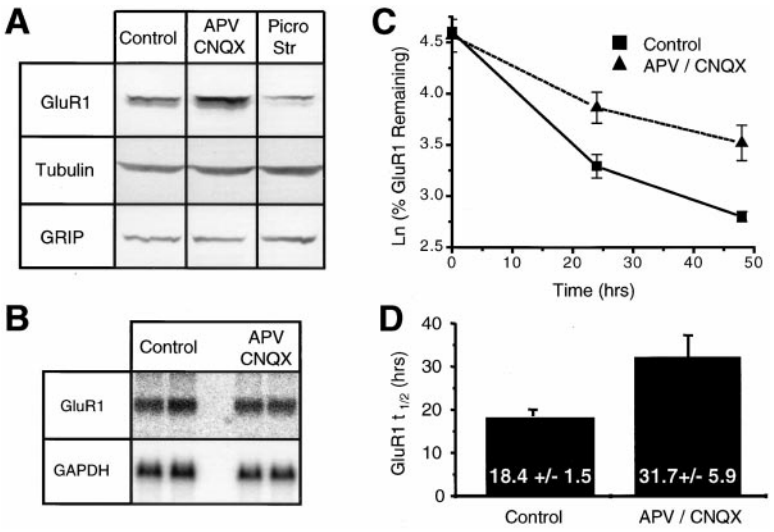

Figure 6. Excitatory Synaptic Transmission Regulates the Accumulation and Turnover of GluR1

(A) High-density cultures of rat spinal neurons (control, active, and inhibited) were taken up in sample buffer, and an equal volume from each was immunoblotted with antibodies to GluR1 and GRIP. The level of synaptic activity had a reciprocal effect on the level of GluR1 protein. Reprobing the same blot with a monoclonal anti-tubulin antibody shows the specificity of this effect. The level of GRIP is unchanged in control and inhibited cultures and is slightly increased in active cultures.

(B) A Northern blot on duplicate control and inhibited (APV and CNQX) spinal cultures is shown. Equivalent amounts of total RNA were run per lane. The GluR1 transcript was approximately 5.5 kb in size, while the GAPDH transcript was 1.6 kb.

(C) The time course for ^{35}S GluR1 degradation in control and inhibited spinal cord cultures (± SEM).

(D) The calculated metabolic half-life (± SD) of ^{35}S GluR1 in control and inhibited spinal cord cultures (n = 4).

distribution of the AMPA receptor–associated protein GRIP (Dong et al., 1997).

Discussion

We have shown that the regulation of synaptic activity in spinal neurons results in a long-term modulation of excitatory synaptic transmission. Inhibition of excitatory synaptic transmission with glutamate receptor antagonists results in an increase in mEPSC amplitudes and kainate sensitivity, presumably to compensate for a reduction in excitatory input. Conversely, an increase in excitatory synaptic activity results in a compensatory decrease in mEPSC amplitudes. To investigate the mechanism underlying this observation, we used a combined approach of measuring mEPSCs and quantitating AMPA receptor cluster size. While a number of mechanisms could account for the alterations in mEPSC size in these cultures, our data suggest that the change in mEPSC amplitudes can be accounted for by an alteration in postsynaptic AMPA receptor accumulation, without a change in the number of excitatory synapses. The time course of this effect was similar to the half-life of normal receptor turnover and was associated with a corresponding change in total receptor amount, without an effect on receptor subunit mRNA levels. These observations, along with our demonstrated reduction in the metabolic half-life of GluR1 by synaptic activity, are most consistent with an activity-dependent destabilization of synaptic AMPA receptors, mediated either by a posttranslational modification of AMPA receptor subunits or by a change in their association with synaptic

Table 3. Synaptic Activity Specifically Increases GluR1 Protein Accumulation without a Change in GluR1 mRNA

The Effect of Synaptic Activity on the Accumulation of GluR1			
	Picro/Str	Control	CNQX/APV
GluR1	0.58 ± 0.11*	1.0 ± 0.15	1.40 ± 0.11*
Tubulin	1.10 ± 0.17	1.0 ± 0.13	0.93 ± 0.19
GluR1/Tubulin	0.53 ± 0.17*	1.0 ± 0.07*	1.48 ± 0.23*
GRIP	1.21 ± 0.17	1.0 ± 0.10	1.04 ± 0.14
Total protein	308 ± 36 μg	327 ± 39 μg	298 ± 32 μg
The Effect of APV and CNQX on GluR1 mRNA Accumulation			
		Control	CNQX/APV
GluR1		1.0 ± 0.14	0.77 ± 0.15
Total RNA		24 ± 5 μg	19 ± 2 μg
Ratio GluR1/GAPDH		1.0 ± .06	0.94 ± .04

High-density control, inhibited, or active cultures grown in 60 mm dishes were solubilized in sample buffer for immunoblotting or had their RNA extracted for Northern blotting as described in Experimental Procedures. After processing, protein bands corresponding to GluR1, GRIP, or tubulin, and mRNA bands corresponding to GluR1 and GAPDH were quantitated using ImageQuant. For immunoblotting, equivalent percentages of a dish were run, while for Northern blotting equivalent amounts of RNA were run. GluR1 and tubulin data points represent six total dishes from three experiments, except for the picrotoxin/strychnine data, which represent four dishes from two platings. The GRIP data and the Northern blots represent three dishes from two platings. Differences from control at the 0.05 level are indicated with an asterisk. Data are expressed relative to control ± SD. The ratios of GluR1/Tubulin protein and GluR1/GAPDH mRNA were calculated using corresponding signals from the same lanes. Total protein (n = 4) and total RNA (n = 3) are expressed per 60 mm dish.

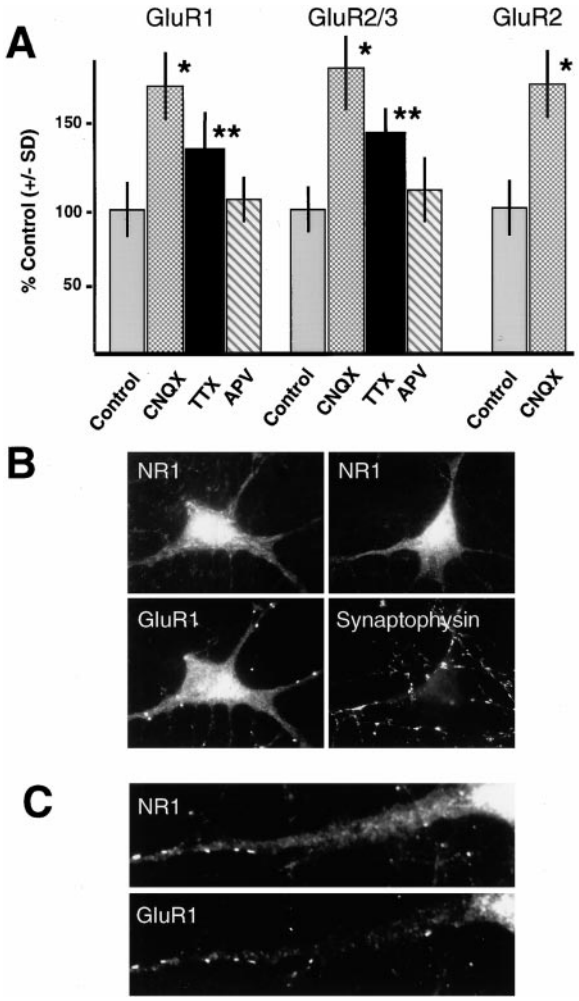

Figure 7. The Role of AMPA and NMDA Receptor Activation in the Synaptic Accumulation of Glutamate Receptors

(A) Spinal neurons were grown for 7 days in control media and then switched to the indicated media for the next 72 hr. Cells were subsequently fixed and stained with the C-GluR1, C-GluR2/3, or GluR2 antibody to measure total synaptic AMPA receptor subunit fluorescence. Each bin represents the mean summed neuronal synaptic fluorescence intensity obtained from 15–20 neurons in two distinct platings and is displayed ± SD. Only CNQX and TTX caused an increase in the synaptic accumulation of both GluR1, GluR2, and GluR2/3 ($p < 0.001$ [CNQX]; $p < 0.05$ [TTX]).

(B) Neurons were grown for 7 days in control medium and then switched to media containing CNQX (10 μM) for 72 hr. The cultures were then fixed and stained for NR1 and either synaptophysin or GluR1. The lack of effect of CNQX on NMDA receptor distribution is revealed by a failure to detect any significant synapse specific localization of the common NMDA receptor subunit NR1.

(C) The effect of APV on the distribution of NMDA receptors within a subpopulation of spinal neurons is shown.

cytoskeletal proteins. Previous work at both the neuromuscular junction (Berg and Hall, 1975; Avila et al., 1989) and at central glutamatergic synapses (Mammen et al., 1997) has shown that the synaptic aggregation of ionotropic receptors is associated with a prolongation of their metabolic half-life. Our work suggests that the effect of innervation on the metabolic turnover of AMPA receptors is further modulated by ongoing synaptic activity. While the majority of our work involved blocking both AMPA and NMDA receptors, it appears that AMPA receptor activation played a predominant role in their own synaptic accumulation without any effect on the accumulation of NMDA receptors. The precise mechanism by which AMPA receptor activation affects their synaptic recruitment is unclear, but it does not appear to be dependent on calcium-permeable AMPA receptors, a redistribution of the synapse-associated protein GRIP, or voltage-dependent sodium channels. Although we saw no change in the presynaptic vesicle protein synaptophysin, our data do not exclude the possibility of other activity-dependent changes in vesicular glutamate release. The particular homeostatic mechanism observed in cultured spinal neurons may be dictated by a lack of any activity-dependent changes in the number of synapses, a phenomenon that has been observed in other systems (Constantine-Paton and Cline, 1998).

The distribution of fluorescence intensities for individual synaptic AMPA receptor clusters fits a rightward-skewed Gaussian distribution that remains unaltered by modulating synaptic activity. Thus, it would appear that normal or moderately increased levels of spontaneous synaptic activity do not qualitatively affect the distribution of AMPA receptors at synapses in cultured spinal neurons. In addition, the ratio of surface to total synaptic GluR1 receptors was not changed by synaptic activity and followed a true Gaussian distribution in all conditions. This suggests that the surface redistribution of a subsurface pool of receptors was not responsible for the increase in synaptic GluR1 accumulation. The Gaussian distribution of the ratio of surface to total synaptic GluR1 subunits also suggests that multiple distinct subpopulations of synapses with variable surface components are not likely to exist in these cultures. Finally, we saw no evidence that the surface distribution of postsynaptic AMPA receptors could be altered on a time scale more rapid than their half-life, even in the face of an abrupt onset of significant excitatory activity. Although our approach did not utilize accepted paradigms for eliciting LTP, it was at least clear that generalized synaptic activity did not cause a short-term change in synaptic AMPA receptor distribution or in the number of AMPA receptor clusters.

It has been widely observed that central excitatory and inhibitory synapses exhibit large variations in their response to quanta of neurotransmitter. In individual neurons this variation is delineated by skewed mEPSC amplitude histograms that are not well described by a Gaussian distribution (see Jack et al., 1994; Walmsley, 1995). It has recently been reported that the large variability of mIPSC amplitudes in individual cerebellar stellate cells closely parallels the variability in immunogold labeling of $GABA_A$ receptors at their synapses (Nusser et al, 1997). This finding suggests that variability in mIPSC amplitudes arises from differences in the number of postsynaptic receptors activated by the quantal release of GABA. It is therefore noteworthy that our skewed mEPSC amplitude histograms, either in individual neurons or in groups of neurons, are matched by a similar skew in the histograms of postsynaptic AMPA receptor cluster intensities. This implies that a limiting number of postsynaptic receptors may account for quantal variability at central excitatory synapses and further suggests that changes in receptor number would directly

affect mEPSC amplitudes. This model is based on the assumption that synaptic glutamate concentrations are near saturation (Bruns and Jahn, 1995).

The fact that long-term synaptic activity (or its inhibition) has an effect on AMPA receptor accumulation at excitatory synapses lends support to the idea that a homeostatic feedback loop adjusts neuronal output to restore the original gain and threshold for plasticity of the postsynaptic neuron (Bear, 1995; Miller, 1996). In the present set of experiments, we have pharmacologically simulated an increase or reduction in the level of postsynaptic activity. A reduction in excitatory synaptic activity results in an increase in postsynaptic AMPA receptor accumulation, larger mEPSCs, and presumably a lower threshold for LTP induction. Conversely, a chronic increase in synaptic activity results in a reduction in postsynaptic AMPA receptor clusters and mEPSC amplitudes over a nearly 3-fold range. While our experiments have involved global effects on synaptic gain, our data do not exclude the possibility that localized increases in synaptic input could initiate localized compensations, which would offset short-term changes in synaptic efficacy. Indeed, the inability of TTX to completely mimic CNQX suggests that mEPSPs can control the scaling of central synapses to some degree, and that voltage-gated sodium channel inhibition is not sufficient to reproduce the effect of synaptic blockade. Whether these mEPSPs are acting locally or globally will be the subject of future work.

Activity-dependent scaling of synaptic input has been recently described in systems as diverse as the *Drosophila* neuromuscular junction (Davis and Goodman, 1998) and cultured mammalian hippocampal and cortical neurons (Lissin et al., 1998; Turrigiano et al., 1998). At the *Drosophila* neuromuscular junction, hyperinnervation leads to a decrease in neurotransmitter release, while a decrease in innervation leads to an increase in quantal size, possibly by altering postsynaptic glutamate receptor sensitivity or number. In cultured cortical neurons, decreases in the level of synaptic activity lead to compensatory increases in postsynaptic glutamate chemosensitivity, while hyperinnervation leads to a reduction in the size of mEPSCs (Liu and Tsien, 1995). We demonstrate that in cultured spinal neurons the activity-dependent change in mEPSC size can be accounted for by an alteration in the stability of postsynaptic AMPA receptors. The mechanisms underlying this effect will offer further insight into the basis for ongoing synaptic plasticity.

Experimental Procedures

Cell Culture

Techniques for culturing rat spinal neurons at both low and high density have been described previously (O'Brien et al., 1997). In these experiments we used P2-4 rat pups as the source of spinal neurons rather than the E17-19 neurons described earlier, and we used 4% rather than 2% horse serum in the growth medium. With cultures from older rats, synapse formation occurs more rapidly and robustly than with embryonic neurons. Autaptic connections are rare under these circumstances (R. J. O. and R. L. H., unpublished observations). For experiments involving chronic inhibition of excitatory synaptic currents, TTX (2 μM), APV (300 μM), CNQX (10 μM), or both APV and CNQX were added to high- or low-density cultures as a 2× concentrate in glial conditioned growth medium on day 7 in vitro. After an additional 36 hr, 50% of the media was changed and replaced with an equal amount of a 1× concentrate of inhibitors in glial conditioned medium. Control cultures were treated with an identical amount of fresh glial conditioned media, lacking the inhibitors. For experiments involving increased excitatory synaptic activity, picrotoxin (final concentration 100 μM) and strychnine (final concentration 2 μM) were added in a similar fashion for 72 hr. Glial conditioned culture media was obtained by incubating standard growth media in a 10 cm dish with cultured spinal glia for at least 6 hr. This preincubation greatly reduced the chances of glutamate-induced toxicity both in basal cultures and in those withdrawn from glutamate receptor antagonists. After a 72 hr incubation in TTX, APV and CNQX, or picrotoxin and strychnine, cultures were processed for immunohistochemistry, electrophysiology, or biochemistry as described below. In several instances, cultures treated with inhibitors for 72 hr were returned to fresh glial conditioned medium without inhibitors for various lengths of time. Control cultures were subjected to the same media changes plus or minus the inhibitors as appropriate. Similar to our previously published data (O'Brien et al., 1997), TTX, APV, and CNQX maintain a complete and prolonged blockade of both sodium channels and excitatory synaptic activity when used in this manner.

Quantitative Immunofluorescence

The antibodies used in this study, N-GluR1, C-GluR1, and C-GluR2/3, are rabbit anti-peptide antibodies raised against the extracellular N terminus of GluR1, the C terminus of GluR1, and the common C terminus of GluR2 and GluR3, respectively, and have been studied extensively in cultured spinal neurons (Mammen et al., 1997; O'Brien et al., 1997). Each recognizes a single protein on immunoblots, and all immunohistochemical signal is blocked by preincubation with appropriate peptide. Techniques for using two rabbit antibodies simultaneously (N-GluR1 and C-GluR1 or C-GluR1 and NR1) have also been established (O'Brien et al., 1997; Mammen et al., 1997). Prior control experiments using blocking peptides have demonstrated no cross-talk between the two rabbit antibodies (Mammen et al., 1997). AMPA receptor subunit antibodies were used at saturating concentrations, defined as a concentration at which a 5-fold excess does not cause an increase in synapse specific staining. For C-GluR1, C-GluR2/3, and N-GluR1, this was between 5 and 10 μg/ml. The monoclonal antibody against synaptophysin (used at a dilution of 1:50) was purchased from Boehringer-Mannheim. A rabbit anti-peptide NR1 antibody, which also specifically recognizes a single appropriately sized band on immunoblots of spinal neurons, was generated against the N terminus of NR1 and was used as described (Kim et al., 1998). A monoclonal antibody against GluR2 (Vissavajjhala et al., 1996), which also shows specific reactivity only for GluR2 in cultured spinal neurons, was used at a concentration of 3 μg/ml, which was a saturating dose as defined above.

Quantitative immunofluorescence was performed using a 100× objective on a Zeiss Axiophot microscope, equipped with a Princeton Instruments cooled CCD camera. Data were acquired using Metamorph acquisition and analysis software (Universal Imaging Corp.). Synaptic AMPA receptor clusters were collected either in a randomized consecutive fashion to avoid ascertainment bias (Figures 3, 5, and 7) or on the basis of selecting neurons with the most synaptic AMPA receptor clusters (Figures 2 and 4). Additionally, in one of the platings reported in Figure 3, the examiner was blinded to the experimental conditions. All methods of data acquisition gave identical results. Images were illuminated three times for 5 s each to acquire the FITC, CY3 (or Rhodamine), and AMCA signals. For triple label experiments (Figures 2, 3, and 4), these corresponded to N-GluR1 (N-terminal, extracellular GluR1; applied to live neurons to stain only surface receptors), C-GluR1 (C-terminal, intracellular GluR1; applied to fixed and permeabilized neurons to stain all synaptic receptors), and synaptophysin, respectively. For double label experiments (Figures 3, 5, and 7), these images corresponded to GluR2, GluR2/3, C-GluR1, or N-GluR1 (rhodamine) and synaptophysin (FITC) signals. In all cases where a comparison was to be made between active, control, and inhibited neurons, an equal number of neurons in each category was digitized for each plating. All experiments involved neurons equally distributed between at least two platings. The 12-bit acquisition range of the Princeton Instrument

camera was adequate for the entire range of synaptic fluorescence intensities, and no neutral density filters were necessary.

Following acquisition, neurons were analyzed with an invariant setting for both contrast (50% system maximum) and brightness (80% system maximum). With these settings, all pixels were well within the linear range of the Metamorph system. Dendrites running through the center of the field were outlined and the threshold adjusted to visually encompass all synaptic AMPA receptor clusters. The presence of synaptophysin ensured that only synaptic GluR1 clusters were analyzed. The total fluorescence intensity and size (pixels) of the clusters were then determined and the diffuse dendritic stain was subtracted to yield the synapse specific intensity. In addition, the ratio of FITC/CY3 (N-GluR1/C-GluR1) at each synaptic cluster was also determined when appropriate. Finally the image was converted to an 8-bit image and printed using Adobe Photoshop. Using these techniques, combined with rigorously standardized staining protocols, we found that variation in the mean synaptic GluR1 fluorescence intensity between neurons on different coverslips within the same plating (approximately 15%) or between platings (approximately 30%) allowed us to sum data across multiple experiments. In generating histograms of individual synaptic fluorescence intensities (Figure 4), data were gathered from a single coverslip to minimize staining-induced variation.

While we found total synaptic fluorescence to be the most convenient and stable method of quantitating synaptic glutamate receptor concentration, the mean peak fluorescence (determined by calculating the mean value of the brightest four pixels within a cluster) also gave a useful quantitative assessment of synaptic GluR1 concentration. Data were expressed as the summed neuronal mean synaptic fluorescence intensities, except in Figures 2, 4, and 5D where individual synaptic fluorescence intensities were evaluated. Coincident with the quantitative immunofluorescence, we performed a series of control experiments on most platings to ensure that the inhibition of synaptic activity had no effect on the number of total synapses or the number of excitatory synapses. For these experiments we used a 63× objective, which allowed us to visualize the entire dendritic arbor of individual neurons. Neurons were stained with CY3-labeled GluR1 and FITC-labeled synaptophysin as described (O'Brien et al., 1997), and the number of total and GluR1 positive synapses per neuron was assessed until we had accumulated ten GluR1 positive neurons per plating. In addition the number of total neurons per 63× field was counted to assess the possibility of differential cell death. All immunohistochemical data are expressed ± SD unless otherwise stated.

Electrophysiology

Whole-cell patch-clamp recordings were made from spinal cord neurons using an Axopatch 200 amplifier (Axon Instruments). Coverslips containing spinal cord cells were mounted in a chamber on an Axiovert 35 microscope (Zeiss). These cells were continuously superfused with a bathing solution composed of (mM): NaCl (150), KCl (2.8), $CaCl_2$ (2), $MgCl_2$ (1), and HEPES (10). The intracellular solution contained (mM): KCl (140), EGTA (5), HEPES (10), tetraethylammonium (2), and Mg^{2+}-ATP (2). The pH of the external and internal solutions was adjusted to 7.3 using NaOH and KOH, respectively. Patch-clamp electrodes were fabricated from borosilicate glass and had resistances of ~2 MΩ after fire polishing. In order to isolate AMPA receptor–mediated mEPSCs, recordings were made in the presence of tetrodotoxin (1.0 μM), picrotoxin (100 μM), strychnine (1 μM), and APV (50 μM). All recordings were made at room temperature (23°C) at a holding potential of −70 mV. MEPSCs and whole-cell kainate-evoked responses were filtered at 2 kHz and acquired at 4 kHz directly onto the hard disc of a personal computer using pClamp (Axon Instruments). MEPSCs were analyzed off-line using an event-fitting program kindly supplied by Dr. Steve Traynelis (Emory University). On average, 50–100 mEPSCs were fitted from each cell in order to obtain mean kinetic and amplitude parameters. All electrophysiologic values presented here represent the mean ± SEM. Comparison of mean values was carried out using a Student's t test and considered significant at the $p < 0.05$ level.

Immunoblotting

Cell lysates from 60 mm dishes containing high-density spinal cord cultures treated for 72 hr with APV, CNQX, APV plus CNQX, picrotoxin plus strychnine, or control media were solubilized in 400 μl SDS/PAGE sample buffer and subjected to SDS-PAGE (7.5% acrylamide). Proteins were transferred to Immobilon-P (Millipore Corp.), immunoblotted using the C-GluR1, C-GluR2/3, and NR1 antibodies (described above) at approximately 0.5 μg/ml, and visualized with enhanced chemiluminescence (ECL, Amersham Corp.). Blots were subsequently stripped at 55°C and reprobed with a monoclonal anti-tubulin antibody (T-9026; Sigma) at a 1:15,000 dilution. Protein band intensity was quantitated using a Molecular Dynamics Personal Densitometer SI and ImageQuantTM software (Mammen et al., 1997).

Northern Blotting

Total RNA was isolated from high-density control and inhibited (APV and CNQX) spinal cultures on day 10, using the Totally RNA kit from Ambion. Five micrograms of each of three control and three inhibited cultures was precipitated overnight with ethanol. Following centrifugation and brief drying, the samples were prepared and fractionated on a 1.1 M formaldehyde/1.3% agarose gel as described (Rosen et al., 1990). Following separation, the samples were transferred to MagnaGraph Nylon (MSI, Inc.; Westborough, MA), UV cross-linked, and then baked in vacuo for 2 hr at 70°C. The blot was hybridized with a 630 bp ACC1 fragment of the 5′ end of the GluR1 cDNA (Heinemann, GenBank #17184) labeled by random priming with ^{32}P dCTP (3000 Ci/mmol; NEN, Boston MA) and the "Prime-It" kit (Stratagene). Following hybridization the blot was washed to high stringency and then exposed to a phosphoimager plate, scanned on a Storm 840 Imager (Molecular Dynamics), and quantitated using ImageQuant. Control coverslips run in parallel with the Northern blots showed the expected increase in immunofluorescent synaptic GluR1. Blots were subsequently stripped and reprobed with a 500 bp fragment of rat GAPDH.

Metabolic Labeling of GluR1

Metabolic labeling of day 10 cultured spinal neurons was performed as described in Mammen et al. (1997) except that 1.5 mCi per dish of Tran^{35}S-label (ICN) was used, and the time points were 0, 24, and 48 hr. Fifty percent media changes with either control or APV/CNQX-containing media were continued every 36 hr during the incubation period. Two separate experiments were performed, each in duplicate, giving identical results. These experiments were combined to create Figures 6C and 6D.

Acknowledgments

This work was supported by a Wellcome Traveling Research Fellowship (S. K.), a grant from the Cal Ripken–Lou Gehrig Fund for Neuromuscular Research, and National Institutes of Health grants K08NS01652 (R. J. O.) and R01NS36715 (R. L. H.). We would like to thank Dr. Dezhi Liao for helpful discussions and for the use of his NR1 antibody.

Received May 22, 1998; revised September 9, 1998.

References

Avila, O., Drachman, D.B., and Pestronk, A. (1989). Neurotransmission regulates stability of acetylcholine receptors at the neuromuscular junction. J. Neurosci. *9*, 2902–2906.

Bear, M. (1995). Mechanism for a sliding synaptic modification threshold. Neuron *15*, 1–4.

Berg, D., and Hall, Z.W. (1975). Loss of alpha-bungarotoxin from junctional and extrajunctional acetylcholine receptors in rat diaphragm muscle in vivo and in organ culture. J. Physiol. *252*, 771–789.

Bruns, D., and Jahn, R. (1995). Real time measurement of transmitter release from single synaptic vesicles. Nature *377*, 62–65.

Choi, D., Farb, D., and Fischbach, G.D. (1981). GABA-mediated synaptic potentials in chick spinal cord and sensory neurons. J. Neurophysiol. *45*, 632–643.

Cline, H.T., and Constantine-Paton, M. (1990). NMDA receptor agonists and antagonists alter retinal ganglion cell arbor structure in the developing frog retinotectal projection. J. Neurosci. *10*, 1197–1216.

Constantine-Paton, M., and Cline, H.T. (1998). LTP and activity-dependent synaptogenesis: the more alike they are the more different they become. Curr. Opin. Neurobiol. *8*, 139–148.

Davis, G.W., and Goodman, C.S. (1998). Synapse specific control of synaptic efficacy at the terminals of a single neuron. Nature *392*, 82–86.

Dong, H.D., O'Brien, R.J., Fung, E., Lanahan, T., Worley, P., and Huganir, R.L. (1997). GRIP, a synaptic PDZ domain containing protein which interacts with AMPA receptors. Nature *386*, 279–284.

Furshpan, E.J., and Potter, D.D. (1989). Seizure-like activity and cellular damage in rat hippocampal neurons in cell culture. Neuron *3*, 199–207.

Hollmann, M., and Heinemann, S. (1994). Cloned glutamate receptors. Annu. Rev. Neurosci. *17*, 31–108.

Jack, J.J.B., Larkman, A.U., Major, G., and Straford, K.J. (1994). Quantal analysis of the synaptic excitation of CA1 hippocampal pyramidal neurons. In Molecular and Cellular Mechanisms of Neurotransmitter Release, L. Stjarne, P. Greengard, S. Grillner, T. Hokfelt, and D. Ottoson, eds. (New York: Raven Press), pp. 275–299.

Kim, J.H., Liao, D., Lau, L.F., and Huganir, R.L. (1998). SynGAP: a synaptic RasGAP that associates with the PSD-95/SAP90 protein family. Neuron *20*, 683–691.

Lissin, D.V., Gomperts, S.N., Carroll, R.C., Christine, C.W., Kalman, D., Kitamura, M., Hardy, S., Nicoll, R.A., Malenka, R.C., and von Zastrow, M. (1998). Activity differentially regulates the surface expression of synaptic AMPA and NMDA glutamate receptors. Proc. Natl. Acad. Sci. USA *95*, 7097–7102.

Liu, G., and Tsien, R.W. (1995). Properties of synaptic transmission at single hippocampal synaptic boutons. Nature *375*, 404–408.

Mammen, A.L., Huganir, R.L., and O'Brien, R.J. (1997) Redistribution and stabilization of cell surface glutamate receptors during synapse formation. J. Neurosci. *17*, 7351–7358.

Martin, L.J., Blackstone, C.D., Levey, A.I., Huganir, R.L., and Price, D.L. (1993). AMPA receptor subunits are differentially distributed in rat brain. Neuroscience *53*, 327–358.

Miller, K.D. (1996). Synaptic economics: competition and cooperation in synaptic plasticity. Neuron *17*, 371–374.

Nusser, Z., Cull-Candy, S.G., and Farrant, M. (1997). Differences in synaptic GABA receptor number underlie variation in GABA mini amplitude. Neuron *19*, 697–709.

O'Brien, R.J., and Fischbach, G.D. (1986). Modulation of embryonic chick motoneuron glutamate sensitivity by interneurons and agonists. J. Neurosci. *11*, 3290–3296.

O'Brien, R.J., Mammen, A.L., Blackshaw, S., Ehlers, M.D, Rothstein, J.D., and Huganir, R.L. (1997). The development of excitatory synapses in cultured spinal neurons. J. Neurosci. *17*, 7339–7350.

Patneau, D.K., Wright, P.W., Winters, C., Mayer, M.L., and Gallo, V. (1994). Glial cells of the oligodendrocyte lineage express both kainate and AMPA preferring subtypes of glutamate receptors. Neuron *12*, 357–371.

Rao, A., and Craig, A.M. (1997). Activity regulates the synaptic localization of the NMDA receptor in hippocampal neurons. Neuron *19*, 801–812.

Roche, K.W., O'Brien, R.J., Mammen, A.L., Bernhardt, J., and Huganir, R.L. (1996). Characterization of multiple phosphorylation sites on the AMPA receptor GluR1 subunit. Neuron *16*, 1179–1188.

Rosen, K.M., Lamperti, E.D., and Villa-Komaroff, L. (1990). Optimizing the northern blot procedure. Biotechniques *8*, 398–403.

Rothstein, J.D., Tsai, G., Kuncl, R.W., Clawson, L., Cornblath, D.R., Drachman, D.B., Pestronk, A., Stauch, B.L., and Coyle, J.T. (1990). Abnormal excitatory amino acid metabolism in ALS. Ann. Neurol. *28*, 18–25.

Segal, M.M., and Furshpan, E.J. (1990). Epileptiform activity in microcultures containing small numbers of hippocampal neurons. J. Neurophysiol. *64*, 1390–1399.

Traynelis, S.F., and Wahl, P. (1997). Control of rat GluR6 glutamate receptor open probability by protein kinase A and calcineurin. J. Physiol. *503*, 513–531.

Turrigiano, G., Leslie, K.R., Desai, N., Rutherford, L.C., and Nelson S. (1998). Activity dependent scaling of quantal amplitude in neocortical neurons. Nature *391*, 892–895.

Vissavajjhala, P., Janssen, W.G., Hu, Y., Gazzaley, A.H., Moran, T., Hof, P.R., and Morrison, J.H. (1996). Synaptic distribution of the AMPA-GluR2 subunit and its colocalization with calcium-binding proteins in rat cerebral cortex: an immunohistochemical study using a GluR2-specific monoclonal antibody. Exp. Neurol. *142*, 296–312.

Walmsley, B. (1995). Interpretation of quantal peaks in distributions of evoked synaptic transmission at central synapses. Proc. R. Soc. Lond. *261*, 245–250.